JOURNAL OF GUIDANCE, CONTROL, AND DYNAMICS
Vol. 20, No. 4, July–August 1997

Close-Approach Trajectories in the Elliptic Restricted Problem

Antonio Fernando Bertachini de Almeida Prado
Instituto Nacional de Pesquisas Espaciais, São José dos Campos, São Paulo 12227-010, Brazil

The swing-by maneuver uses a close approach with a celestial body to modify the velocity, energy, and angular momentum of a spacecraft's orbit. The swing-by trajectories are studied and classified under the model given by the elliptic restricted three-body problem. Several simulations are made to show the effects of the eccentricity of the primaries in this maneuver. The position of the secondary in its orbit (specified by its true anomaly) also has effects on the results, and they are quantified. To show the results, the orbit of the spacecraft is classified in four groups: elliptic direct, elliptic retrograde, hyperbolic direct, and hyperbolic retrograde. Then the modification in the orbit of the spacecraft due to the close approach is shown in plots that specify from which group the spacecraft's orbit is coming and to which group it is going. Several families of orbits are found and shown in detail. An analysis about the trends as parameters vary is performed, and the influence of each of them is shown and explained. The results presented can also be used to find optimal sets of parameters for several types of problems, such as finding an escape orbit that has minimum velocity at periapsis and other related problems.

Introduction

THE swing-by maneuver is a very popular technique used to decrease fuel expenditure in space missions. The most common approach to study this problem is to divide it into three phases dominated by two-body celestial mechanics. Another model used to study this problem is the circular restricted three-body problem.[1–3]

In the present paper, the swing-by maneuvers are studied and classified under the model given by the planar elliptic restricted three-body problem. It is assumed that the system is formed by two main bodies that are in elliptic orbits around their center of mass and a massless third body that is moving under the gravitational attraction of the two primaries. This third body has its motion constrained to the orbital plane of the two primaries.

The goal is to simulate a large variety of initial conditions for those orbits and classify them according to the effects caused by the close approach on the orbit of the spacecraft. This close approach is assumed to be performed around the secondary body of the system. Special attention is given to identifying the regions where the captures and escapes occur.

The number of swing-by trajectories around a celestial body is infinite. Thus, to define a specific trajectory, it is necessary to define and to give the numeric values of some variables. To solve this problem, a modified version of the set of variables used in Refs. 1–3 is used here. The three variables (see Fig. 1) are 1) V_p, the velocity of the spacecraft at periapsis of the orbit around the secondary body; 2) ψ, the angle between the line M_1–M_2 (the two primaries) and the direction of the periapsis of the trajectory of the spacecraft around M_2; and 3) r_p, the distance from the spacecraft to the center of M_2 at the moment of closest approach to M_2 (periapsis distance).

For a large number of values of these three variables, the equations of motion are integrated numerically forward and backward in time, until the spacecraft is at a distance that can be considered far enough from M_2. (It is necessary to integrate in both directions of time because the set of initial conditions used gives information about the spacecraft exactly at the moment of the closest approach.) At these two points, the effect of M_2 can be neglected, and the system formed by M_1 and the spacecraft can be considered a two-body system to compute the energy and the angular momentum before and after the close approach. Then, the orbits are classified in four categories: elliptic direct (negative energy and positive angular momentum), elliptic retrograde (negative energy and angular momentum), hyperbolic direct (positive energy and angular momentum), and hyperbolic retrograde (positive energy and negative angular momentum). The convention for the sign of the angular momentum is positive for a counterclockwise orbit and negative for a clockwise orbit. Then the problem is to identify the category of the orbit of the spacecraft before and after the close encounter with M_2. After this classification is made, it is possible to identify up to 16 classes of transfers, according to the changes in the category of the orbit caused by the close encounter. They are named with the first 16 letters of the alphabet.

Using a large number of simulations, it is possible to understand the influence of each parameter and improve our understanding of this problem. Also, several optimal problems involving this maneuver can be formulated and solved with the help of the plots shown. Some examples include finding specific types of orbits (escape, capture, etc.) that have maximum or minimum velocity at periapsis (or any other parameters, such as the distance of the periapsis or the angle of approach). A section of this paper shows the possibilities.

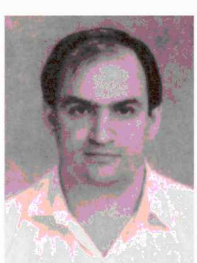

Antonio F. B. A. Prado is a Research Engineer and Professor in the Space Mechanics and Control Division at the National Institute for Space Research (INPE) in Brazil. He received the following academic degrees: Ph.D. (1993) and M.S. (1991) in Aerospace Engineering from the University of Texas at Austin, Texas; M.S. in Space Science (1989) from INPE; and B.S. in Physics (1986) and Chemical Engineering (1985) from the University of Sao Paulo, Brazil. He is a Senior Member of the AIAA and a member of the Tau-Beta-Pi National Engineering Honor Society and of the Honor Society of Phi-Kappa-Phi. He is the author of several papers in celestial mechanics with emphasis on orbital maneuvers.

Received June 17, 1996; revision received March 3, 1997; accepted for publication March 10, 1997.

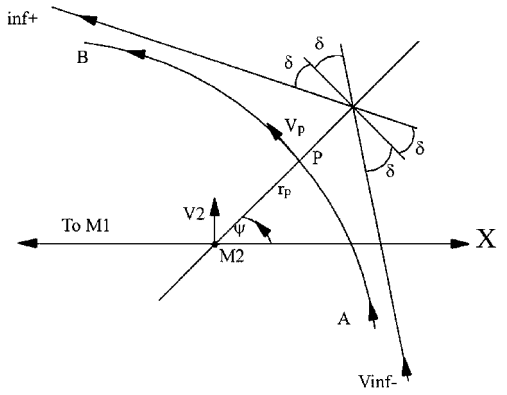

Fig. 1 Standard swing-by maneuver.

Standard Swing-By Maneuver

The standard swing-by maneuver consists of using a close encounter with a celestial body to change the velocity, energy, and angular momentum of a smaller body (an orbit of a comet or a spacecraft). This maneuver can be identified by three independent parameters: 1) $V_{\text{inf}-}$, the magnitude of the velocity of the spacecraft when approaching the celestial body, or V_p, the magnitude of the velocity of the spacecraft at periapsis (these quantities are related by a single equation, which means that if one of them is specified, the other can be obtained); 2) r_p, the distance between the spacecraft and the celestial body during the closest approach; and 3) ψ, the angle of approach (angle between the periapsis line and the line that connects the two primaries). Figure 1 shows the sequence for this maneuver.

It is assumed that the system has three bodies: a primary (M_1) and a secondary (M_2) body with finite mass that are in circular orbit around their common center of mass and a third body with negligible mass (the spacecraft) that has its motion governed by the two other bodies. The spacecraft goes from point A to point B. Points A and B are chosen in such a way that the influence of M_2 at those points can be neglected and, consequently, the energy is constant after B and before A (the system spacecraft–M_1 follows two-body celestial mechanics). The result of this maneuver is a change in velocity, energy, and angular momentum in the Keplerian orbit of the spacecraft with respect to M_1. Using the patched conic approximation, the equations that quantify those changes are available in the literature.[1] The most important equations are

$$\delta = \sin^{-1}\left[\frac{1}{1+\left(r_p V_{\text{inf}}^2/\mu_2\right)}\right] \tag{1}$$

$$\Delta V = 2V_{\text{inf}}\sin\delta \tag{2}$$

$$\Delta E = \omega \Delta C = -2V_2 V_{\text{inf}}\sin\delta\sin\psi \tag{3}$$

In these equations, δ is half of the total deflection of the trajectory of the spacecraft (see Fig. 1), V_2 is the linear velocity of M_2 in its motion around the center of mass of the system M_1–M_2, ω is the angular velocity of the M_1–M_2 system, C is the angular momentum of the spacecraft's orbit, and μ_2 is the gravitational parameter of M_2. Examining these equations, it is possible to get the fundamental well-known results as follows. 1) The variation in energy ΔE is equal to the variation in angular momentum ΔC [Eq. (3)] because the angular velocity ω is unity in the reference system used. 2) If the flyby is in front of the secondary body, there is a loss of energy, and this loss has a maximum at $\psi = 90$ deg. 3) If the flyby is behind the secondary body, there is a gain of energy, and this gain has a maximum at $\psi = 270$ deg.

There are many studies of the standard swing-by maneuver in different missions. Some examples are the study of missions to the satellites of the giant planets,[4] new missions to Neptune[5] and Pluto,[6] and the study of the Earth's environment.[7,8]

Elliptic Restricted Problem

For the research performed, the equations of motion for the spacecraft are assumed to be given by the well-known planar restricted elliptic three-body problem. The standard dimensionless canonical system of units is used: the unit of distance is the semimajor axis of the orbit of M_1 and M_2 with respect to each other; the mean angular velocity ω of the motion of M_1 and M_2 is assumed to be unity; the mass of the smaller primary (M_2) is given by $\mu = m_2/(m_1 + m_2)$, where m_1 and m_2 are the real masses of M_1 and M_2, respectively, and the mass of M_1 is $(1-\mu)$; the unit of time is defined such that the period of the motion of the two primaries is 2π; and the gravitational constant of the M_1–M_2 system [the product of the universal constant of gravitation $G = 6.67 \times 10^{-11}$ m^3/(kg · s^2) and the total mass of the system] is unity.

There are several systems of reference that can be used to describe the elliptic restricted three-body problem.[9,10] In this section, the fixed (inertial) and the rotating-pulsating systems are described. Figure 2 shows these systems in detail.

In the fixed system, the origin is located in the center of mass of the two heavy masses M_1 and M_2. The horizontal axis $\bar{x}$ is the line connecting M_1 and M_2 (at the initial time), and the vertical axis $\bar{y}$ is perpendicular to $\bar{x}$. In this system, M_1 and M_2 follow elliptic trajectories given by the equations $\bar{x}_1 = -\mu r\cos\nu$, $\bar{y}_1 = -\mu r\sin\nu$, $\bar{x}_2 = (1-\mu)r\cos\nu$, and $\bar{y}_2 = (1-\mu)r\sin\nu$, where r is the distance between the two primaries, given by the expression $r = (1-e^2)/(1+e\cos\nu)$, and ν is the true anomaly of M_2. In this system, the equations of motion of the massless particle are

$$\ddot{\bar{x}} = \frac{-(1-\mu)(\bar{x}-\bar{x}_1)}{r_1^3} - \frac{\mu(\bar{x}-\bar{x}_2)}{r_2^3} \tag{4}$$

$$\ddot{\bar{y}} = \frac{-(1-\mu)(\bar{y}-\bar{y}_1)}{r_1^3} - \frac{\mu(\bar{y}-\bar{y}_2)}{r_2^3} \tag{5}$$

where the double overdots are the second derivative with respect to time and r_1 and r_2 are the distances between the spacecraft and M_1 and M_2, respectively, given by the expressions

$$r_1^2 = (\bar{x}-\bar{x}_1)^2 + (\bar{y}-\bar{y}_1)^2 \qquad r_2^2 = (\bar{x}-\bar{x}_2)^2 + (\bar{y}-\bar{y}_2)^2$$

In the rotating-pulsating system of reference, the origin is again the center of mass of the two massive primaries. The horizontal axis x is the line that connects the two primaries all of the time. It rotates with a variable angular velocity to follow the trajectory of M_1 and M_2 in such a way that the two massive primaries are always on this axis. The vertical axis y rotates with the same angular velocity to stay perpendicular to the x axis. Besides the rotation, the system also pulsates in such a way to keep the massive primaries in fixed positions. To achieve this situation, it is necessary to multiply the unit of distances by the instantaneous value of the distance between the two primaries (r). In this system, the positions of the primaries are $x_1 = -\mu$, $x_2 = 1-\mu$, and $y_1 = y_2 = 0$. In this way, the unit of distance is not fixed in time, but it changes as the distance between the primaries modifies. In this system of

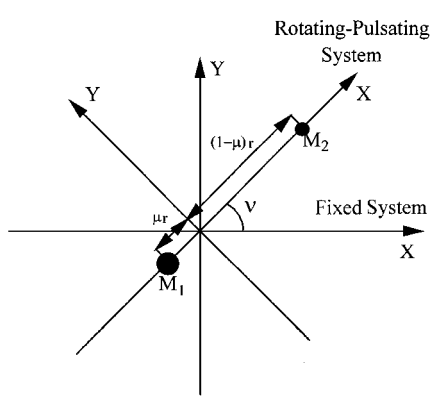

Fig. 2 Fixed and rotating-pulsating reference systems.

reference, the equations of motion for the massless particle are

$$x'' - 2y' = (r/p)\left\{x - (1-\mu)\left[(x-x_1)/r_1^3\right] - \mu\left[(x-x_2)/r_2^3\right]\right\} \tag{6}$$

$$y'' + 2x' = (r/p)\left[y - (1-\mu)\left(y/r_1^3\right) - \mu\left(y/r_2^3\right)\right] \tag{7}$$

(Ref. 9), and there is also an equation to relate time and the true anomaly of the primaries, given by

$$t' = r^2/p^{\frac{1}{2}} \tag{8}$$

where the prime represents a derivative with respect to the true anomaly of the primaries and $p[=a(1-e^2)]$ is the semilatus rectum of the ellipse.

The equations that relate one system to another are

$$\bar{x} = rx\cos\nu - ry\sin\nu \tag{9}$$

$$\bar{y} = rx\sin\nu + ry\cos\nu \tag{10}$$

$$x = \frac{\bar{x}\cos\nu + \bar{y}\sin\nu}{r} \tag{11}$$

$$y = \frac{\bar{y}\cos\nu - \bar{x}\sin\nu}{r} \tag{12}$$

for the positions and

$$\dot{\bar{x}} = \dot{x}r\cos\nu - \dot{y}r\sin\nu - \frac{x(1-e^2)\sin\nu}{(1+e\cos\nu)^2} - \frac{y(1-e^2)(e+\cos\nu)}{(1+e\cos\nu)^2} \tag{13}$$

$$\dot{\bar{y}} = \dot{x}r\sin\nu + \dot{y}r\cos\nu - \frac{y(1-e^2)\sin\nu}{(1+e\cos\nu)^2} + \frac{x(1-e^2)(e+\cos\nu)}{(1+e\cos\nu)^2} \tag{14}$$

$$\dot{x} = \frac{\dot{\bar{x}}\cos\nu}{r} + \frac{\dot{\bar{y}}\sin\nu}{r} - \frac{\bar{x}(\sin\nu + e\sin 2\nu)}{1-e^2} + \frac{\bar{y}(\cos\nu + 2e\cos^2\nu - e)}{1-e^2} \tag{15}$$

$$\dot{y} = \frac{\dot{\bar{y}}\cos\nu}{r} - \frac{\dot{\bar{x}}\sin\nu}{r} - \frac{\bar{y}(\sin\nu + e\sin 2\nu)}{1-e^2} - \frac{\bar{x}(\cos\nu + 2e\cos^2\nu - e)}{1-e^2} \tag{16}$$

for the velocities.

Algorithm to Solve the Problem

A numerical algorithm to solve the problem has the following steps.

1) Arbitrary values for the three parameters r_p, V_p, and ψ are given.

2) With these values, the initial conditions in the fixed system are computed. The initial position is the point (X_i, Y_i) and the initial velocity is (V_{Xi}, V_{Yi}), where

$$X_i = (1-\mu)r\cos(\nu) + r_p\cos(\psi + \nu) \tag{17}$$

$$Y_i = (1-\mu)r\sin(\nu) + r_p\sin(\psi + \nu) \tag{18}$$

$$V_{Xi} = V_r\cos(\nu) - V_t\sin(\nu) - V_p\sin(\psi + \nu) \tag{19}$$

$$V_{Yi} = V_r\sin(\nu) + V_t\cos(\nu) + V_p\cos(\psi + \nu) \tag{20}$$

where V_r and V_t are the radial and transverse components of the velocity of the secondary body with respect to an inertial frame. They are calculated by

$$V_r = \frac{(1-\mu)e\sin\nu}{\sqrt{1-e^2}} \tag{21}$$

$$V_t = \frac{(1-\mu)(1+e\cos\nu)}{\sqrt{1-e^2}} \tag{22}$$

3) With these initial conditions, the equations of motion are integrated forward in time until the distance between M_2 and the spacecraft is larger than a specified limit d. At this point, the numerical integration is stopped and the energy E_+ and the angular momentum C_+ after the encounter are calculated.

4) Then the particle is reset to its initial conditions at the point P, and the equations of motion are integrated backward in time until the distance d is reached again. Then the energy E_- and the angular momentum C_- before the encounter are calculated.

For all of the simulations shown, a fourth-order Runge–Kutta method with stepsize control was used for numerical integration. The criterion to stop the numerical integration is the distance between the spacecraft and M_2. When this distance reaches the value $d = 0.5$ (half of the semimajor axis of the two primaries), the numerical integration is stopped. The value 0.5 is a lot larger than the sphere of influence of M_2, that is, 0.00077, which avoids any important effects of M_2 at these points. Simulations using larger values for this distance were performed, and the integration time was increased but the results were not significantly changed. To study the effects of numerical accuracy, several cases were simulated using different integration methods and/or different values for the accuracy required with no effects in the results. All of the calculations were performed with an IBM-PC computer (Pentium 100 MHz) using the Microsoft Fortran power station compiler.

With this algorithm available, the given initial conditions (values for r_p, V_p, and ψ) are varied in any desired range, and the effects of the close approach in the orbit of the spacecraft are studied.

Results

The results consist of plots that show the change of the orbit of the spacecraft due to the close encounter with M_2. First, it is necessary to classify all of the close encounters between M_2 and the spacecraft, according to the change obtained in the orbit of the spacecraft. The 16 letters A–P are used for this classification. They are assigned to the orbits according to the rules shown in Table 1.

After defining the meaning of the letters, the results consist of assigning one of those letters to a position in a two-dimensional diagram that has the parameter ψ (in degrees) on the horizontal axis and the parameter V_p (in canonical units) on the vertical axis. This type of diagram is called a letter plot, and it was used in Ref. 1. In the present paper, 12 combinations of eccentricity and ν are shown in Figs. 3–5. For all of these plots, the following parameters are used: $\mu = 0.0121$, $d = 0.5$, and $r_p = 0.00495$ canonical units. For each plot, a total of 961 trajectories were generated, dividing each axis into 31 segments. The interval plotted for ψ is $180 < \psi < 360$ deg because there is a symmetry with respect to the vertical line $\psi = 180$ deg. The plot for the interval $0 < \psi < 180$ deg is a mirror image of the region $180 < \psi < 360$ deg with the following letter substitutions: L becomes O, N becomes H, I becomes C, B becomes E, M becomes D, and J becomes G. K, P, F, and A remain unchanged.

By examining Figs. 3–5, it is possible to identify the following families of orbits. 1) Orbits that result in an escape (transfer from elliptic to hyperbolic) are represented by the letters I, J, M, and N and appear in an inclined stripe close to the center of the plots. 2) Orbits that result in a capture (transfer from hyperbolic to elliptic) are represented by the letters C, D, G, and H and occur only for $e = 0.4$ and $\nu = 270$ deg in the plots shown. They are located in the upper-left-hand part of the plots. 3) Elliptic orbits (transfer from elliptic to elliptic) are represented by the letters A, B, E, and F and are at the bottom left of the plots. 4) Hyperbolic orbits (transfer from hyperbolic to hyperbolic) are represented by the letters K, L, O, and

Table 1 Rules to assign letters to orbits

	After			
Before	Direct ellipse	Retrograde ellipse	Direct hyperbola	Retrograde hyperbola
Direct ellipse	A	E	I	M
Retrograde ellipse	B	F	J	N
Direct hyperbola	C	G	K	O
Retrograde hyperbola	D	H	L	P

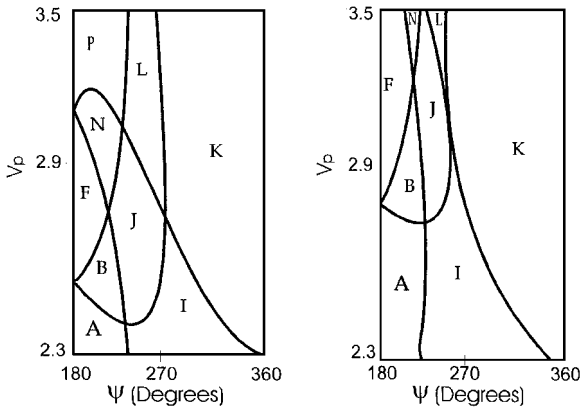

$e = 0.0$ and $\nu = 0$ deg

$e = 0.4$ and $\nu = 0$ deg

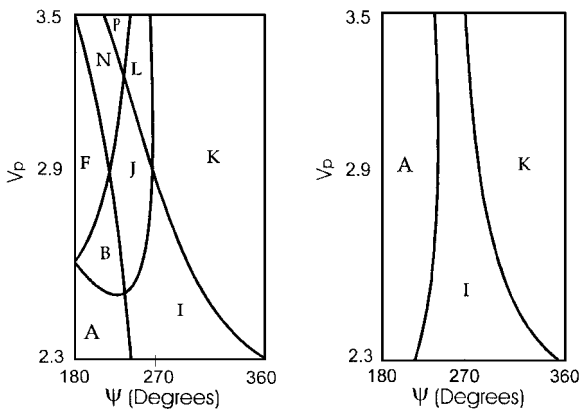

$e = 0.2$ and $\nu = 0$ deg

$e = 0.8$ and $\nu = 0$ deg

Fig. 3 Effects of the eccentricity of the primaries.

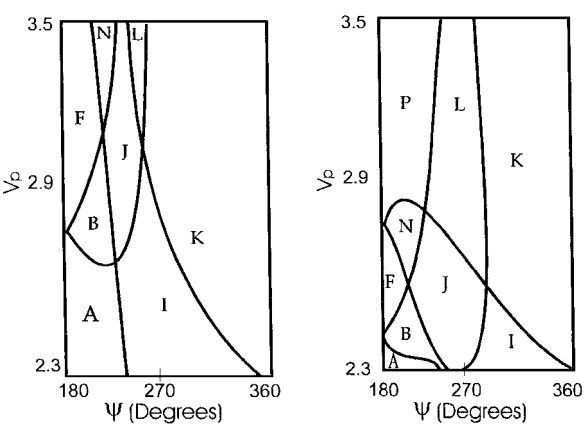

$e = 0.4$ and $\nu = 0$ deg

$e = 0.4$ and $\nu = 180$ deg

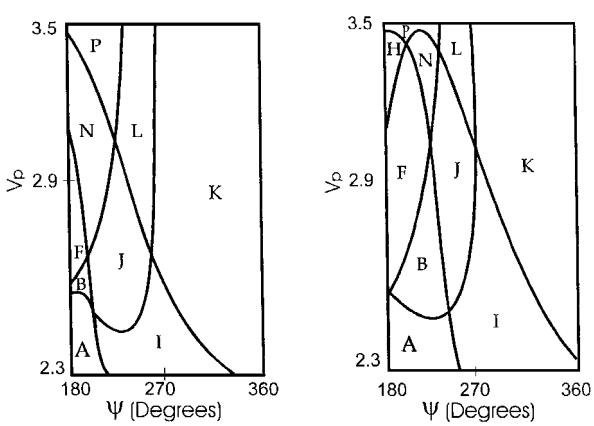

$e = 0.4$ and $\nu = 90$ deg

$e = 0.4$ and $\nu = 270$ deg

Fig. 4 Effects of the true anomaly of the primaries.

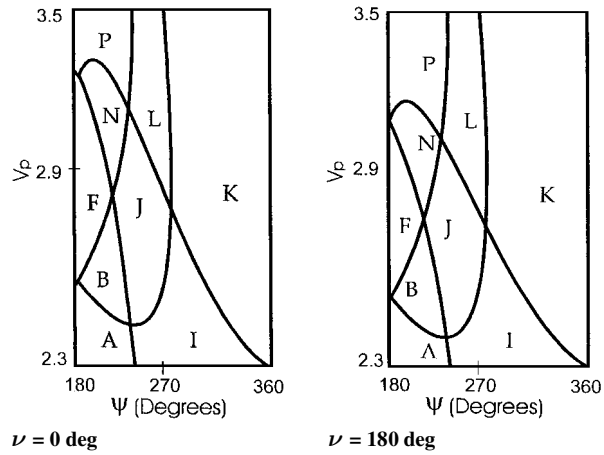

$\nu = 0$ deg

$\nu = 180$ deg

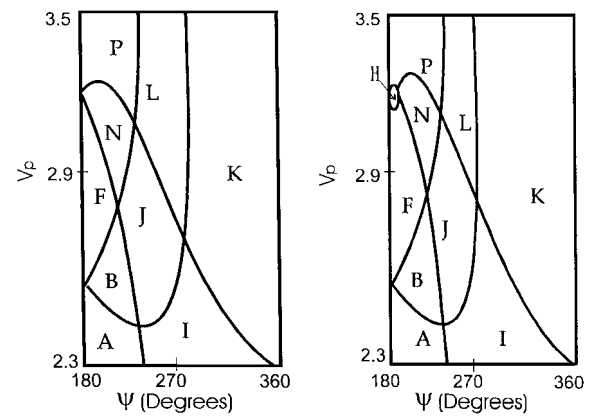

$\nu = 90$ deg

$\nu = 270$ deg

Fig. 5 Results for the Earth–moon system.

P and are at the upper right of the plots. 5) Orbits that change the direction of motion from direct to retrograde are represented by the letters E, M, G, and O and appear in an inclined stripe in the upper center of the part of the plots that is not shown ($0 < \psi < 180$ deg). 6) Orbits that change the direction of motion from retrograde to direct are represented by the letters B, D, J, and L and appear in an inclined stripe in the upper center of the plots. 7) Retrograde orbits are represented by the letters F, H, N, and P and appear in the upper left of the plots. 8) Direct orbits are represented by the letters A, C, I, and K and appear in the bottom right of the plots. Of course, there are the mirror images for the interval $0 < \psi < 180$ deg for all of the plots, with the substitutions given earlier.

The borderlines between those families are also interesting families of orbits. The borders that separate elliptic from hyperbolic orbits are made by parabolic orbits. Examples of borders that have parabolic orbits after the close approach are A–I, B–J, F–N, and H–P. Examples of borders that have parabolic orbits before the close approach are I–K, J–L, N–P, N–L, and F–H. The borders that separate direct from retrograde orbits represent orbits with zero angular momentum. In this case, position and velocity are parallel (rectilinear orbits). Examples of borders that have zero angular momentum after the close approach are F–B, N–J, and L–P. Examples of borders that have zero angular momentum before the close approach are K–L, I–J, and A–B. It is easy to see those families. In a general way, a typical plot can be divided into three regions with respect to the energy (elliptic to elliptic, elliptic to hyperbolic, hyperbolic to hyperbolic) and three regions with respect to the angular momentum (retrograde to retrograde, direct to retrograde, direct to direct). The final format is a result of the intersections of these regions.

Trends as Parameters Vary

The restricted elliptic three-body problem has very few analytical results available in the literature. One of the best alternatives to improve the knowledge of this problem is to combine numerical

simulations with the analytical results that come from the patched-conic approximation. In this section, these tools are used to study the trends as parameters vary in the close-approach maneuver.

The parameters that govern the system under study are the eccentricity of the primaries (e), the true anomaly of M_2 in its orbit around M_1 (ν), the angle of approach of the swing-by (ψ), the periapsis distance r_p, and the velocity at periapsis V_p.

Effects of the Eccentricity of the Primaries

Figure 3 shows the effect of the eccentricity for a fixed true anomaly ($\nu = 0$ deg). The values used for the eccentricity are 0.0, 0.2, 0.4, and 0.8. Many important points are visible. Captures occur only in the part not shown ($0 < \psi < 180$ deg). Escapes occur in all cases, but the occurrence of case I increases with the eccentricity up to the point of dominating exclusively for $e = 0.8$. Transfers between hyperbolic orbits occur in all cases, but the occurrence of case K increases with the eccentricity up to the point that P is eliminated when $e = 0.4$ and L is eliminated when $e = 0.8$. Transfers between elliptic orbits also occur in all cases, but the occurrence of case A increases with the eccentricity up to the point that B and F are both eliminated when $e = 0.8$. The increase of the eccentricity of the primaries (keeping the other parameters fixed) causes an increase of the velocity of $M_2(V_2)$ at the periapsis of its orbit around M_1. This fact comes from the equation of energy for a system of two bodies: velocity at periapsis (because $\nu = 0$ deg) is

$$V_2 = \sqrt{G(m_1 + m_2)\left[\frac{2}{a(1-e)} - \frac{1}{a}\right]}$$

By examining Eq. (3), it is easy to see that the variation in energy ΔE is proportional to V_2. Therefore, the general effect of increasing the eccentricity of the primaries is to increase ΔE when $\nu = 0$ deg (and to decrease ΔE when $\nu = 180$ deg).

Effects of the True Anomaly of $M_2(\nu)$

Figure 4 shows the effect of the true anomaly for a fixed eccentricity ($e = 0.4$). The values used for the true anomaly are 0, 90, 180, and 270 deg. Some of the important points (in the region $180 < \psi < 360$ deg) are as follows. Captures occur only for $\nu = 270$ deg; escapes occur in all cases but in a reduced quantity when $\nu = 180$ deg; and the distribution among all of the letters changes considerably. Thus, the main influence of this parameter is to change the velocity V_2. V_2 increases when M_2 moves to the periapsis, and it causes an increase in the effects of the swing-by. It is easy to see that the area of escapes/captures decreases and increases accordingly.

Effects of the Angle of Approach ψ

The behavior of the angle of approach follows very closely the prediction of the patched-conic approximation. The maximum effect in the maneuver occurs close to $\psi = 270$ deg (and $\psi = 90$ deg, in consequence). The most interesting trajectories (captures and escapes) are in that region. Close to the borders of the plots ($\psi = 180$ and 360 deg), there are only trajectories with little or no effects from the swing-by (elliptic-elliptic and hyperbolic-hyperbdic). The angle ψ also has an influence on the definition of the type of the orbit. Following a line of constant V_p (so that all of the parameters are fixed except ψ), note that for $\psi \approx 180$ deg (the spacecraft is between the primaries), the orbit is initially elliptic. For $\psi \approx 360$ deg (the spacecraft is at the opposite side of M_1, when viewed from M_2), the orbit is initially hyperbolic.

Effects of the Periapsis Distance r_p

The effects of the periapsis distance are also very easy to understand. When this parameter decreases, the effects in the maneuver increase and the area of interesting orbits (captures/escapes) becomes larger. Conversely, increasing the periapsis distance makes the area of trivial trajectories (elliptic to elliptic, hyperbolic to hyperbolic, etc.) increase. Several simulations (not shown, to save space) were performed and confirmed this prediction.

Effects of the Periapsis Velocity

The velocity at periapsis plays an important role in this maneuver. The limits for this variable come in a very natural way. If values below a certain lower limit are used, the spacecraft is captured by M_2 and the swing-by does not occur. If values above a certain upper limit are used, the ΔE increases [see Eq. (3)], but the orbit before and after the maneuver becomes hyperbolic and the families K, P, and L dominate the plots. These limits change from situation to situation, but in general they are close to 2.30 in the lower side and 3.50 in the upper side. For values slightly above the lower limit, the orbits are usually elliptic before and/or after the maneuver, as they are for the families A, B, J, and I that dominate the bottom part of the plots. Also note that there is a minimum value for this velocity that allows a change in the sign of the angular momentum.

Optimization Problems

The study has an important application for mission designers. From the plots produced, it is possible to find an optimal set of variables, subject to possible restrictions, to achieve some specific goals. It is usual in mission analyses to have problems such as finding a swing-by that generates a certain desired trajectory (a posigrade escape, a retrograde capture, etc.) with the requirement of having a maximum or minimum in one or more parameters. In particular, V_p and r_p are parameters that may be required to be extremized. If the goal is to collect data from M_2, it is interesting to minimize r_p (to get closer to M_2) and V_p (to maximize the duration of the flyby). Conversely, if M_2 represents a risk to the spacecraft due to the presence of an atmosphere, radiation, etc., it is necessary to maximize r_p and/or V_p, subject to the restriction of obtaining the desired change in the trajectory.

To use a real case as an example, Fig. 5 shows the plots for the Earth–moon system with the moon in four possible locations ($\nu = 0$, 90, 180, and 270 deg). All of the comments made in the preceding sections for Figs. 3 and 4 apply and are not repeated. In the remainder of this section, two examples of problems of optimization are studied.

Problem 1

It is desired to get a trajectory type N (a retrograde escape) in the Earth–moon system, subject to the constraint $r_p = 1903$ km and requiring that the velocity at periapsis be a minimum. By examining Fig. 5, it is possible to see that the trajectories of type N that have minimum V_p for each plot are $V_p = 2.90$ for $\nu = 0$ deg, $V_p = 2.82$ for $\nu = 90$ deg, $V_p = 2.82$ for $\nu = 180$ deg, and $V_p = 2.86$ for $\nu = 270$ deg. Then, any of the trajectories with $V_p = 2.82$ ($\nu = 90$ or 180 deg) solves the problem. Figure 6 shows the real trajectory of the spacecraft in the fixed system of reference for the case $\nu = 90$ deg.

Problem 2

It is desired to get a trajectory that is a retrograde ellipse after the swing-by (types E, F, G, and H) in the Earth–moon system, subject to the constraint $r_p = 1903$ km and requiring that the velocity at periapsis be a maximum. By examining Fig. 5, it is possible to see that the trajectories of the types desired that have maximum V_p for each plot are $V_p = 3.26$ for $\nu = 0$ deg, $V_p = 3.14$ for $\nu = 90$ deg, $V_p = 3.10$ for $\nu = 180$ deg, and $V_p = 3.14$ for $\nu = 270$ deg. All of these trajectories are of type F. Then, the trajectory with $V_p = 3.26$ ($\nu = 0$ deg) is the solution of the problem. Figure 6 shows the real trajectory of the spacecraft in the fixed system of reference.

Improvements that can be made in this study include the following. 1) More plots can be generated for different values of ν to have more information; and 2) r_p can be a free parameter and, in this case, plots for several values of r_p must be generated to find the optimal trajectory. Many other types of optimization problems can be solved using the method developed. For a given system of primaries, the eccentricity is fixed but the other four parameters are potentially free and can be used to improve the performance of the mission. Systems of primaries in circular orbits have one fewer parameter (ν), but they can also benefit from this technique to solve optimal problems.

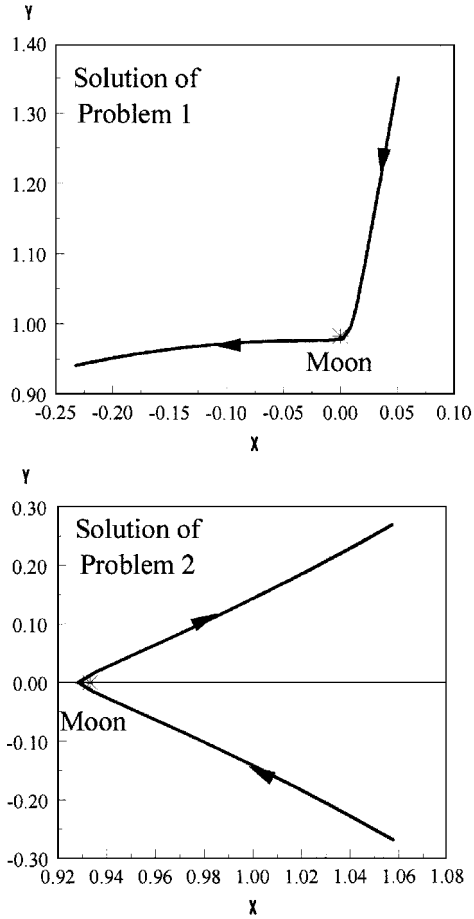

Fig. 6 Trajectories in the Earth–moon system.

Conclusions

The elliptic restricted three-body problem is described and used to study the swing-by maneuver. Several letter plot graphics are made to represent the effect of a close approach in the orbit of a spacecraft. In particular, the effects of the eccentricity of the primaries and the true anomaly of M_2 in its trajectory around M_1 in this maneuver are studied. It is shown that (when $e = 0.4$) a value of 270 deg for the true anomaly allows captures to occur in the region $180 < \psi < 360$ deg and a value of 180 deg reduces the occurrence of escapes. It is also shown that the increase of the eccentricity causes an increase of the size of three classes of orbits (A, I, and K) and a reduction of the size of all of the other families. For $e = 0.8$, these classes dominate exclusively. Families with peculiarities such as parabolic or zero angular momentum orbits are shown to exist in the borders between the main families. In general, it is clear that the eccentricity of the primaries and the true anomaly of the secondary at the moment of closest approach both play a very important role in the problem under investigation. A study of the influence of the other parameters was also performed, and the results showed a close agreement with the patched-conic prediction. After that, an important application of the present study was made to solve problems that require an extremization of one or more parameters, keeping restrictions in others. Example problems such as finding a certain type of trajectory with fixed r_p and that maximizes or minimizes V_p were solved to show the utilization of the method developed.

Acknowledgments

The author is grateful to the National Council for Scientific and Technological Development, Brazil, for the research grant received under Contract 300221/95-9 and to the Foundation to Support Research in the São Paulo State for the research grant received under Contract 1995/9290-1.

References

[1]Broucke, R. A., "The Celestial Mechanics of Gravity Assist," AIAA Paper 88-4220, Aug. 1988.

[2]Broucke, R. A., and Prado, A. F. B. A., "Jupiter Swing-By Trajectories Passing Near the Earth," *Space Flight Mechanics*, edited by R. G. Melton, L. J. Wood, R. C. Thompson, and S. J. Kerridge, Vol. 82, Pt. 2, Advances in the Astronautical Sciences, American Astronautical Society, Pasadena, CA, 1993, pp. 1159–1176.

[3]Prado, A. F. B. A., "Optimal Transfer and Swing-By Orbits in the Two- and Three-Body Problems," Ph.D. Dissertation, Dept. of Aerospace Engineering and Engineering Mechanics, Univ. of Texas, Austin, TX, Dec. 1993.

[4]D'Amario, L. A., Byrnes, D. V., and Stanford, R. H., "Interplanetary Trajectory Optimization with Application to Galileo," *Journal of Guidance, Control, and Dynamics*, Vol. 5, No. 5, 1982, pp. 465–471.

[5]Swenson, B. L., "Neptune Atmospheric Probe Mission," AIAA Paper 92-4371, Aug. 1992.

[6]Weinstein, S. S., "Pluto Flyby Mission Design Concepts for Very Small and Moderate Spacecraft," AIAA Paper 92-4372, Aug. 1992.

[7]Farquhar, R. W., and Dunham, D. W., "A New Trajectory Concept for Exploring the Earth's Geomagnetic Tail," *Journal of Guidance, Control, and Dynamics*, Vol. 4, No. 2, 1981, pp. 192–196.

[8]Farquhar, R., Muhonen, D., and Church, L. C., "Trajectories and Orbital Maneuvers for the ISEE-3/ICE Comet Mission," *Journal of Astronautical Sciences*, Vol. 33, No. 3, 1985, pp. 235–254.

[9]Broucke, R. A., "Stability of Periodic Orbits in the Elliptic, Restricted Three-Body Problem," *AIAA Journal*, Vol. 7, No. 6, 1969, pp. 1003–1009.

[10]Szebehely, V., *Theory of Orbits*, Academic, New York, 1967, Chap. 10.